

# **Fabrication of coconut shell-derived porous carbons for CO<sub>2</sub> adsorption application**

## **(Supplementary materials)**

Jiali Bai<sup>a</sup>, Jiamei Huang<sup>a</sup>, Qiyun Yu<sup>a</sup>, Muslum Demir<sup>b</sup>, Eda Akgul<sup>b</sup>, Bilge Nazli Altay<sup>c, d</sup>, Xin Hu<sup>\*, a</sup>, Linlin Wang<sup>\*, e</sup>

<sup>a</sup>Key Laboratory of the Ministry of Education for Advanced Catalysis Materials, Zhejiang Normal University, Jinhua, Zhejiang, 321004, PR China

<sup>b</sup> Department of Chemical Engineering, Osmaniye Korkut Ata University, Osmaniye 80000, Turkiye

<sup>c</sup>College of Engineering Technology, Print and Graphic Media Science, Rochester Institute of Technology, Rochester, NY, United States

<sup>d</sup> Institute of Pure and Applied Sciences, Marmara University, Goztepe, Istanbul 34722, Turkiye

<sup>e</sup>Key Laboratory of Urban Rail Transit Intelligent Operation and Maintenance Technology and Equipment of Zhejiang Province, College of Engineering, Zhejiang Normal University, Jinhua, Zhejiang, 321004, PR China

\*Corresponding author's e-mail: huxin@zjnu.cn (X. H.), wanglinlin@zjnu.cn (L. W.); phone: 86-151-0579-0257; fax: 86-579-8228-8269.

## **Synthesis**

In a typical preparation, coconut shell (CS) was mixed with a KOH aqueous solution to achieve KOH/CS mass ratios of 0.3:1, 0.5:1, and 1:1. After thorough stirring, the blend was put into a convection oven with the temperature 120 °C

overnight. Afterward, the achieved slurry mixture was put into a tubular furnace under the protection of N<sub>2</sub> flow. First, the temperature was elevated to and kept at 200 °C for 1 h and then further raised to the designed activation temperature (700, 750, or 800 °C). The resulting samples were rinsed multiple times with distilled water until the pH value of filtrate reached 7. Then, the as-obtained samples were heated at 150 °C under vacuum for 24 h. The resultant carbonaceous sorbents were designated as CSC-T-m; T and m are the activation temperature and the KOH/CS mass ratio, respectively.

### **Characterization**

Powdered X-ray diffraction (XRD) patterns were carried out on a PHILIPS PW3040/60 powder diffractometer using CuK $\alpha$  radiation ( $\lambda = 0.15406\text{nm}$ ). Scanning electron microscopy (SEM Hitachi S-4800) was used to observe the morphology of the samples of carbon materials. Further details of the pore structure were determined by transmission electron microscopy (TEM, JEOL-2100F) operated at 200 kV. The CHN elements were analyzed using a VarioEL III Elemental Analyzer. Nitrogen adsorption and desorption isotherms were measured on a Beishide 3H-2000PS2 sorption analyzer at -196°C. Ultrahigh-purity N<sub>2</sub> (99.999%, Shanghai Pujiang Gas Co., Ltd) was used for measurement. Before measurement, the samples were degassed in a vacuum at 200°C for at least 12h. The specific surface area ( $S_{BET}$ ) was calculated according to the multipoint Brunauer-Emmett-Teller (BET) method from the adsorption data in the relative pressure range between 0.001 and 0.01. The total micropore volume ( $V_t$ ) was deduced from the N<sub>2</sub> adsorption data by the t-plot method,

and the total pore volume ( $V_0$ ) was estimated from the adsorbed amount of liquid nitrogen at a relative pressure of 0.99. The pore size distribution was calculated using the density functional theory (DFT) method. In addition, X-ray photoelectron (XPS) measurements were performed using an AXIS Nova spectrometer (Kratos Inc., NY, USA) equipped with a monochromatic Al K $\alpha$  X-ray source (1486.6 eV). XPS survey spectra were recorded with a pass energy of 160 eV, and high-resolution spectra with a pass energy of 40 eV. A non-linear least squares curve fitting program (Peak-Fit version 4) with a Gaussian-Lorentzian mix function and Shirley background subtraction was used to deconvolve the XPS subpeaks.

The CO<sub>2</sub> adsorption isotherms were measured using the Beshide 3H-2000PS2 sorption analyzer at 0°C and 25°C, respectively. Pure CO<sub>2</sub> (99.99%, Shanghai Pujiang Gas Co., Ltd) was used for adsorption. Prior to each adsorption experiment, the sample was degassed for 12 h at 200°C to remove the guest molecules from the pores. The volume of narrow micropores (with sizes <1 nm),  $V_n$ , was calculated from CO<sub>2</sub> adsorption at 0°C using the Dubinin–Radushkevich (D-R) equation. The measurements were repeated for each sample, until the values fell within  $\pm 2\%$  of each other.

### **Measurement of dynamic CO<sub>2</sub> uptake of the sorbents**

The dynamic CO<sub>2</sub> uptake of the sorbents was tested on a fixed-bed reactor schematically illustrated in Scheme S1 at 1 bar and 25 °C. First, sample was heated at 100°C for 1 h under N<sub>2</sub> at a flow rate of 20 mL/min. The gas flow was shifted from nitrogen to a 10% mixture of CO<sub>2</sub> in N<sub>2</sub> at a flow rate of 10 mL/min, when the sample

temperature was lowered to 25°C. The effluent gases were monitored online using an Agilent 7820A gas chromatograph with a thermal conductivity detector (TCD) to obtain the breakthrough curve.

The dynamic CO<sub>2</sub> uptake of the sorbent ( $q_d$ ) was calculated from the breakthrough curves using the following equation:

$$q_d = \frac{Q_F C_0 t_s}{w} \quad (1)$$

In the above equation,  $Q_F$  is the feed molar flow rate,  $C_0$  is the concentration of the adsorbate in the feed stream,  $w$  is the weight of the adsorbent materials loaded in the column and  $t_s$  is the stoichiometric time, which can be estimated from breakthrough curves using the equation below:

$$t_s = \int_0^\infty \left( 1 - \frac{C_A}{C_0} \right) \partial t \quad (2)$$

Where  $C_A$  is the adsorbate concentration at the column outlet.

### **Measurement of CO<sub>2</sub> adsorption kinetics**

The adsorption kinetics of CO<sub>2</sub> was measured in a thermogravimetric analyzer (NETZSCH STA 449C). In the kinetic analysis, the sample (~5 mg) was degassed under a He stream at 200°C for 1 h. Next, the temperature was cooled to the experimental temperature of 25°C. Then the CO<sub>2</sub> gas was fed into the test chamber with a flow rate of 50 mL/min and the weight variation with time was recorded.

### **IAST CO<sub>2</sub>/N<sub>2</sub> selectivity**

To calculate the IAST CO<sub>2</sub>/N<sub>2</sub> selectivity, the CO<sub>2</sub> adsorption isotherm was fitted with a Langmuir–Freundlich equation and N<sub>2</sub> isotherm was fitted with a linear equation, respectively.

The adsorption selectivity of carbon dioxide over nitrogen was calculated according to the following equation:

$$S = \frac{V_1/V_2}{P_1/P_2}$$

where V<sub>1</sub> and V<sub>2</sub> are the adsorbed amount of carbon dioxide at 0.1 bar and nitrogen at 0.9 bar, respectively, which can be derived from the fitted equation; P<sub>1</sub> and P<sub>2</sub> are the equilibrium partial pressure of carbon dioxide (0.1 bar) and nitrogen (0.9 bar) in the bulk gas phase, respectively.

### **CO<sub>2</sub> heat of adsorption**

CO<sub>2</sub> heat of adsorption was calculated using a variant of the Clausius-Clapeyron equation taking both the 273K and 298K CO<sub>2</sub> adsorption data.

$$\ln\left(\frac{P_1}{P_2}\right) = Q_{st} * \frac{T_2 - T_1}{R * T_1 * T_2}$$

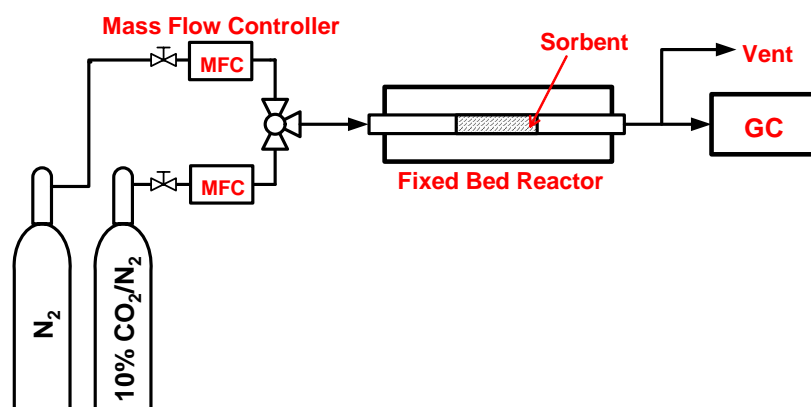
Where P<sub>n</sub> : Pressure for isotherm n

T<sub>n</sub>: Temperature for the isotherm n

R: Gas constant

Pressure as the function of the adsorbed amount was determined by using Langmuir–Freundlich equation. This Langmuir–Freundlich equation gives an accurate fit over the pressure up to 1 bar and with the goodness of fit (R<sup>2</sup>) above 0.99. The corresponding P<sub>1</sub> and P<sub>2</sub> at a certain CO<sub>2</sub> adsorbed amount of both temperatures can be obtained by the simulated Langmuir–Freundlich equation. Then input these

numbers into the above equation, the corresponding CO<sub>2</sub> heat of adsorption was calculated.



Scheme S1. Schematic of the fixed-bed reactor system.

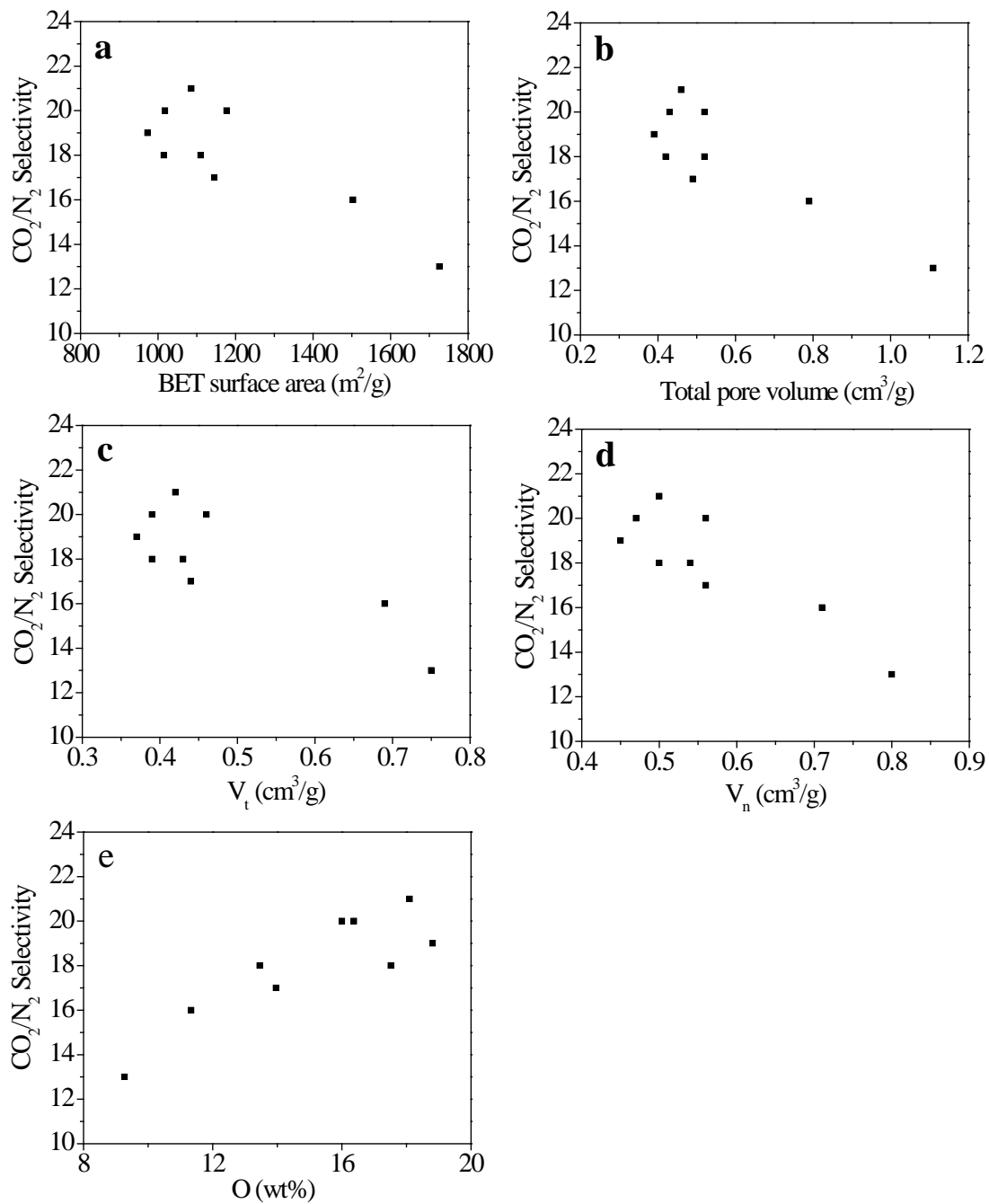


**Figure S1.** Plot of each porous properties characteristics (a)  $S_{\text{BET}}$ , (b)  $V_0$ , (c)  $V_t$ , (d)  $V_n$ , and (e) oxygen content versus CO<sub>2</sub>/N<sub>2</sub> selectivity.

Table S1. Comparison of the CO<sub>2</sub> adsorption (25 °C and 1 bar) for different sorbents

Sample	CO <sub>2</sub> uptake (mmol/g)	Ref.
AA750	2.7	S1
GEPM-1	2.5	S2
GMNO-4	2.6	S3
GTCF-3	2.7	S4
MRF-2	2.5	S5
OM-CNS	3.0	S6
NAC	4.0	S7
PC-700	3.6	S8
CEMFAET	3.8	S9
AC-2-635	3.9	S10
AC1040	4.3	S11
CP-2-600	3.9	S12
CPTHB-7	3.7	S12
Cell-UK	4.4	S13
TOK-900	4.3	S14
MOF-2	0.6	S15
MOF-505	3.3	S16
ZIF-78	2.7	S17
UFC-600-3	3.5	S18
PSK-2-650	3.5	S19
CSC-750-0.5	4.2	This study

## References

- S1. Balahmar, N.; Mitchell, A. C.; Mokaya, R., Generalized Mechanochemical Synthesis of Biomass-Derived Sustainable Carbons for High Performance CO<sub>2</sub> Storage. *Adv. Energy Mater.* **2015**, *5*, (22), 1500867.
- S2. Sui, Z.Y.; Cui, Y.; Zhu, J.H.; Han, B.H., Preparation of Three-Dimensional Graphene Oxide–Polyethylenimine Porous Materials as Dye and Gas Adsorbents. *ACS Appl. Mater. Interfaces* **2013**, *5*, (18), 9172-9179.
- S3. Zhou, D.; Liu, Q.; Cheng, Q.; Zhao, Y.; Cui, Y.; Wang, T.; Han, B.,

Graphene-manganese oxide hybrid porous material and its application in carbon dioxide adsorption. *Chin. Sci. Bull.* **2012**, *57*, (23), 3059-3064.

S4. Zhou, D.; Cheng, Q.Y.; Cui, Y.; Wang, T.; Li, X.; Han, B. H., Graphene-terpyridine complex hybrid porous material for carbon dioxide adsorption. *Carbon* **2014**, *66*, 592-598.

S5. Zhou, H.; Xu, S.; Su, H.; Wang, M.; Qiao, W.; Ling, L.; Long, D., Facile preparation and ultra-microporous structure of melamine-resorcinol-formaldehyde polymeric microspheres. *Chem. Commun.* **2013**, *49*, (36), 3763-3765.

S6. Zheng, L.; Li, W. B.; Chen, J. L., Nitrogen doped hierarchical activated carbons derived from polyacrylonitrile fibers for CO<sub>2</sub> adsorption and supercapacitor electrodes. *RSC Adv.* **2018**, *8*, (52), 29767-29774.

S7. Zhang, Z.; Xu, M.; Wang, H.; Li, Z., Enhancement of CO<sub>2</sub> adsorption on high surface area activated carbon modified by N<sub>2</sub>, H<sub>2</sub> and ammonia. *Chem. Eng. J.* **2010**, *160*, (2), 571-577.

S8. Chen, C.; Yu, Y.; He, C.; Wang, L.; Huang, H.; Albilali, R.; Cheng, J.; Hao, Z., Efficient capture of CO<sub>2</sub> over ordered micro-mesoporous hybrid carbon nanosphere. *Appl. Surf. Sci.* **2018**, *439*, 113-121.

S9. Fan, X.; Zhang, L.; Zhang, G.; Shu, Z.; Shi, J., Chitosan derived nitrogen-doped microporous carbons for high performance CO<sub>2</sub> capture. *Carbon* **2013**, *61*, 423-430.

S10. Li, D.; Zhou, J.; Zhang, Z.; Li, L.; Tian, Y.; Lu, Y.; Qiao, Y.; Li, J.; Wen, L., Improving low-pressure CO<sub>2</sub> capture performance of N-doped active carbons by adjusting flow rate of protective gas during alkali activation. *Carbon* **2017**, *114*,

496-503.

S11. Plaza, M. G.; Pevida, C.; Martin, C. F.; Feroso, J.; Pis, J. J.; Rubiera, F., Developing almond shell-derived activated carbons as CO<sub>2</sub> adsorbents. *Sep. Purif. Technol.* **2010**, *71*, (1), 102-106.

S12. Xia, Y.; Mokaya, R.; Walker, G. S.; Zhu, Y., Superior CO<sub>2</sub> Adsorption Capacity on N-doped, High-Surface-Area, Microporous Carbons Templated from Zeolite. *Adv. Energy Mater.* **2011**, *1*, (4), 678-683.

S13. Rehman, A.; Nazir, G.; Rhee, K. Y.; Park, S. J., A rational design of cellulose-based heteroatom-doped porous carbons: Promising contenders for CO<sub>2</sub> adsorption and separation. *Chem.Eng. J.* **2021**, *420*, 130421.

S14. Rehman, A.; Heo, Y. J.; Nazir, G.; Park, S. J., Solvent-free, one-pot synthesis of nitrogen-tailored alkali-activated microporous carbons with an efficient CO<sub>2</sub> adsorption. *Carbon* **2021**, *172*, 71-82.

S15. Tian, Z.; Huang, J.; Zhang, X.; Shao, G.; He, Q.; Cao, S.; Yuan, S., Ultra-microporous N-doped carbon from polycondensed framework precursor for CO<sub>2</sub> adsorption. *Microporous Mesoporous Mater.* **2018**, *257*, 19-26.

S16. Millward, A. R.; Yaghi, O. M., Metal-Organic Frameworks with Exceptionally High Capacity for Storage of Carbon Dioxide at Room Temperature. *J. Am. Chem. Soc.* **2005**, *127*, (51), 17998-17999.

S17. Furukawa, H.; Yaghi, O. M., Storage of Hydrogen, Methane, and Carbon Dioxide in Highly Porous Covalent Organic Frameworks for Clean Energy Applications. *J. Am. Chem. Soc.* **2009**, *131*, (25), 8875-8883.

S18. Huang, J.; Bai, J.; Demir, M.; Hu, X.; Jiang, Z.; Wang, L., Efficient N-Doped Porous Carbonaceous CO<sub>2</sub> Adsorbents Derived from Commercial Urea-Formaldehyde Resin. *Energy Fuels* **2022**, 36, (11), 5825-5832.

S19. Zhang, Y.; Wei, Z.; Liu, X.; Liu, F.; Yan, Z.; Zhou, S.; Wang, J.; Deng, S. Synthesis of palm sheath derived-porous carbon for selective CO<sub>2</sub> adsorption, *RSC Adv.* **2022**, 12, 8592-8599.